EUROPEAN COMMISSION

Community Research

# RAPHAEL

**Contract Number: 516508 (FI6O)**


**DELIVERABLE (D-ML3.5)**

# Status of development of modelling method for graphite

Author(s): **Graham HALL**

Reporting period: 15/04/2005 – 14/04/2006

Date of issue of this report : 14/04/2006

Start date of project : **15/04/2005** Duration : **48 Months**

| **Project co-funded by the European Commission under the Euratom Research and Training Programme on Nuclear Energy within the Sixth Framework Programme (2002-2006)** | | |
|---|---|---|
| **Dissemination Level (place an X in the appropriate cell)** | | |
| **PU** | Public | |
| **RE** | Restricted to the partners of the RAPHAEL project | |
| **CO** | Confidential, only for specific distribution list defined on this document | **X** |

# Distribution list

| Person and organisation name and/or group | Comments |
|---|---|
| SP ML WP3 Participants | |
| Sylvie CASALTA, EC DG RTD | |
| Panagiotis MANOLATOS, EC DG RTD | |
| Edgar BOGUSCH, AREVA NP | |
| Vincent CHAUVET, STEP | |
| | |
| | |
| | |
| | |
| | |
| | |
| | |
| | |
| | |
| | |
| | |
| | |
| | |
| | |
| | |
| | |
| | |
| | |

| **ReActor for Process heat, Hydrogen And ELectricity generation (RAPHAEL)** | | |
|---|---|---|
| **Sub-project:** SP-ML<br>**Work package:** 3 | **RAPHAEL document no:**<br>RAPHAEL-0604-D-ML3-5 | **Document type:**<br>D=Deliverable / M=Minute /<br>P=Progress report / S=Support |
| **Issued by:** Uni Man (UK)<br>**Internal no.:** NGRG R170 issue 1 | | **Document status:**<br>Final |

**Document title**

# Status of development of modelling method for graphite

**Abstract**

A task in the Euratom 6th Framework Programme project RAPHAEL is to investigate the use of microstructural modelling methodologies to predict the behaviour of graphite in very high temperature reactor environments. This undertaking has been divided into a number of sub-tasks, of which the first 3 have been completed and are reported here. By applying a range of criteria, nine material properties have been identified and arranged in preferential order of examination; dimensional change, Young's modulus, coefficient of thermal expansion, density, thermal conductivity, irradiation creep, strength, fracture toughness, and Poisson's ratio. A review of possible microstructural modelling approaches, encompassing both the nuclear graphite and general materials research fields, has been conducted. For each of the nine material properties, at least 1 candidate modelling technique has been chosen and will be examined further, applied, and then reassessed in the next stages of the work.

**Revisions**

| Rev. | Date | Short description | Author | WP Leader | SP Leader | Coordinator |
|---|---|---|---|---|---|---|
| 01 | 14/04/2006 | First issue | G Hall, Uni Man | Derek Buckthorpe NNC | Derek Buckthorpe NNC | E.Bogusch, ANP |
| | | | | | | |
| | | | | | | |
| | | | | | | |

# Contents

# 1 Introduction

The European Commission's 6th Euratom Framework Programme (RAPHAEL-IP) incorporates numerous sub-projects that support research co-operation and integration of research efforts in the nuclear fission and fusion area. One such sub-project is the Materials Sub-project (SP-ML). Each of the sub-projects are subdivided into work packages, with Work Package 3 (WP3) of SP-ML being concerned with graphite materials for the very-high temperature reactor (VHTR).

There are 4 tasks within WP3:

- Task 1 – continuation of 750°C irradiation tests.
- Task 2 – graphite irradiation test at higher (>950°C) VHTR temperatures.
- Task 3 – corrosion and heat-up test.
- Task 4 – graphite modelling.

The final task (Task 4) is being undertaken by the University of Manchester and was summarised as[1]:

> *For the longer term development of graphites and to minimise the extent of future irradiation testing, work will also be carried out on an investigation of microscopic modelling methods for prediction and assessment of graphite behaviour making use of micrographs and tomography images of graphites used in the RAPHAEL-IP tests.*

with the added note that it is:

> *essential that its behaviour is fully understood and investigated up to at least the peak dose and over the appropriate temperature ranges.*

The programme designed to achieve Task 4[2] includes the identification and selection of graphite properties to be examined, a survey of possible modelling techniques, a stage report of the first two sub-tasks, the selection of modelling techniques to be used and which graphite it is to be applied to, preliminary application of these techniques, development and re-application of the techniques, and a final report on the task.

This report (Task 4.3) documents the first 3 sub-tasks by first giving some background information. The VHTR designs considered are outlined, including a summary of the operating limits envisaged and thus, the limits of any models. A brief introduction to the computed X-ray tomography technique is also given. The decision as to which graphite properties are to be examined and in what order is discussed in detail, with attention given to what material property data is available or will be available. An examination of possible modelling methods and how the techniques may be or have

been applied to graphite material properties is included. The data requirements in each case are also emphasised. Overall conclusions as to the modelling techniques deemed to be the most promising have been drawn. The future work has been outlined with respect to the development and application of the methods selected.

## 1.1 Very High Temperature Reactors

As the majority of the world strive to develop $CO_2$ and greenhouse-gas free energies, interest in hydrogen as a clean fuel of the future has grown. The Very High Temperature Reactor (VHTR) concept has the potential to offer an efficient, economic and safe means of energy production, and through the use of high temperature process heat, the ability to generate hydrogen. There are currently two categories of VHTRs: prismatic and pebble-bed.

### 1.1.1 Prismatic

In this design the fuel is compacted into small spheres (~ø1mm) and, in order to protect and contain the fission product, coated in layers of carbon and silicon carbide. These particles are then bonded into rods of graphite/resin matrix, which are in turn inserted into hexagonal graphite blocks. The blocks can then be assembled to form the reactor core. Control rod and helium coolant channels are machined into the hexagonal blocks. Experimental reactors of this type have been successfully demonstrated in the UK (DRAGON), the USA (Peach Bottom 1), and Japan currently operate an experimental reactor (HTTR). Only one commercial plant of this type has been operated (Fort St. Vrain, USA).

### 1.1.2 Pebble-bed

A different approach to the VHTR concept was originally designed in Germany; the Arbeitsgemeinschaft Versuchs Reacktoren (Jointly-developed Prototype Reactor) or AVR. The fuel in this design is contained in large graphite spheres (~ø60mm) which are loosely packed in a graphite container, forming the so-called pebble-bed. The container not only acts as a reflector but also houses the normal control rods; additional control rods were forced through the pebble bed from the top. Helium coolant flows downwards preventing the spheres from rising. The fuel spheres move from the top to the bottom of the core, where they are removed, checked for amount of fissile material remaining, and the reinserted if the amount is high enough or replaced if it is not. This means that unlike the prismatic design, the pebble-bed can be refuelled online.

The Thorium Hochtemperatur Reacktor (Thorium High Temperature Reactor) or THTR-300 in Germany commercially exploited this design, although the THTR-300 inserted control rods through the pebbles in the centre of the reactor while the AVR had control rods located in the reflectors. China operates a test facility (HTR-10) and is currently developing a commercial version, and South Africa are working on a modular version of the pebble-bed reactor (PBMR).

### 1.1.3 Operating conditions and limits

In both of the VHTR designs, the normal operating conditions can be considered to be similar (Table 1). The coolant is helium, temperatures are between 400-1100°C, and the maximum dose is 30 dpa ($230 \times 10^{20}$ n/cm$^2$ Equivalent DIDO Nickel). The combination of impurities in the helium and the graphite, the irradiation dose, and the temperature can lead to radiolytic and thermal oxidation of the graphite. These conditions will result in significant graphite dimensional and material property changes with operation of the reactor. It should be noted that some of the graphite components are designed to be removable and usually it will be the changes in the permanent components that are of prime concern.

**Table 1 Operating conditions for a VHTR[3].**

| Operating condition | Limits or description |
|---|---|
| Coolant | helium + impurities ($H_2O$, CO, $CO_2$) |
| Temperature | 400-1100°C |
| Maximum dose | 30 dpa – corresponds to lifetime |
| Oxidation | ~2-3% estimated (radiolytic and thermal, weight loss at end-of-life) |

During accident conditions there is no dose but there may be rapid thermal oxidation due to air or water ingress. In this study, the primary focus is on the normal operating conditions but if possible, the changes in graphite during an accident scenario may also be considered.

## 1.2 Computed X-ray tomography

Although computed X-ray tomography (CT) has been used in the medical field for many years, it has only recently been applied to the study of graphite microstructure. As CT is relatively new and the Work Plan specifically highlights CT as being a source of information for any graphite microstructural models, it may be beneficial to explain the main concepts behind the technique.

Computed X-ray tomography is a non-destructive technique that provides a means to examine the 3D microstructure of a material. In the case of an irradiation programme,

a specimen can be removed for inspection and then placed back in the reactor for further irradiation. The CT technique involves sending an X-ray beam through a sample and recording the transmitted beam using a detector, usually a CCD (charge-coupled device) camera (Figure 1). The ratio of transmitted to incident photons is related to the integral of the absorption coefficient of the material along the path that the photons made through the material[4]. Using an empirical law, the absorption coefficient can be related to the density, the atomic number and in certain cases, the energy. The resulting image is a projection of a volume in a 2D plane. The most popular method to obtain a 3D image is to obtain radiographs whilst rotating the sample between 0° and 180°. An algorithm (filtered back-projection) can then be used to form or reconstruct the volume from the 2D radiographs.

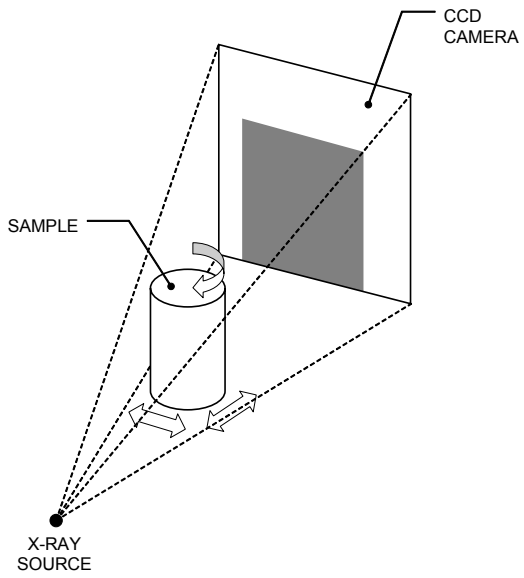


**Figure 1 Schematic of X-ray tomography using a micro-focus X-ray tube source.**

There are two different sources used in X-ray tomography. A micro-focus X-ray tube produces a polychromatic divergent beam whilst a synchrotron radiation source is a able to produce either a polychromatic or monochromatic beam that is parallel to the detector; the micro-focus X-ray tube arrangement is usually found in the smaller scale devices. Depending upon what source is available tomography may be performed in different ways or modes; holotomography mode, phase contrast mode, and absorption mode.

When using an X-ray tube source, the sample is placed between the source and detector. The sample should fit the field of view of the detector, and thus a compromise must often be made between the sample size and the spatial resolution (this also depends upon the detector i.e. number of pixels in the CCD camera). Because the beam is polychromatic (white), quantitive analysis requires calibration and is only accurate in single phase materials.

### 1.2.1 Outputs from tomography

The CT technique has the ability to give a number of characteristics of a sample in a non-destructive way. The porosity can be examined in 3D terms but a number of factors have to be considered. The sample size and CCD camera used affects the resolution of the 3D image. If a ø10mm sample is scanned using a CCD camera with a resolution of 1024 × 1024 pixels, the resulting reconstructed volume will have a resolution of ~11µm i.e. each 3D pixel (a voxel) will be ~11 × 11 × 11µm. Thus, the smallest porosity or characteristics that can be identified will be ~11µm. If however, a smaller sample is used (ø5mm) the voxel size will reduce (~6µm) but the representative volume will have reduced also. It is therefore a trade between sample size and resolution. The resolution may also be increased by having a CCD camera with an increased pixel resolution i.e. 2048 × 2048 pixels.

The results will also be affected by the processing of the reconstructed volume. To separate or segment the volume, a greyscale or threshold value is often used. The value used may not be obvious and may cause uncertainty in the results. For example, the porosity in a sample may be segmented from the bulk material using a threshold value (Figure 2). However, the amount of porosity can be highly dependent upon what value is used.

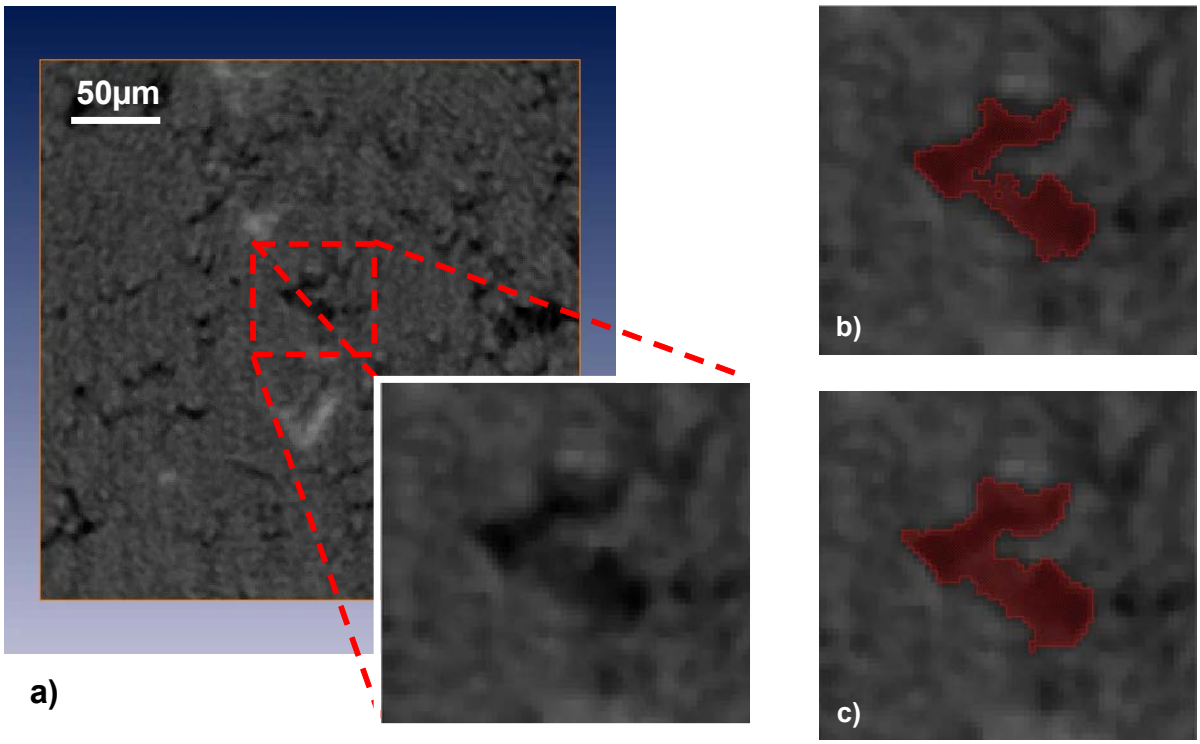


**Figure 2 Effect of threshold value on segmentation process; a) reconstructed 3D volume of a graphite sample (8 bit, 255 greyscale); b) segmentation of pore using threshold value of 36; c) segmentation of pore using threshold value of 42.**

When the sample is single phase, it is possible to obtain the density distribution and bulk density of the sample. This requires calibration of the equipment and material under examination, so that the greyscales in the reconstructed volume can be related to a density value.

# 2 Selection of properties (Task 4.1)

There are numerous graphite properties that could be examined but to make the most efficient usage of time and resources, it was essential that some importance criteria be applied. This selection process highlighted those properties seen to have the greatest beneficial prospects as it may not be possible to examine all of the properties. The first stage of the selection process was to consider what properties would a designer or operator of a VHTR want to be able to predict.

## 2.1 Designers' and operators' requirements

In the reactor, the graphite must fulfil a number of critical functions[3, 5, 6]:

- the graphite must act as a moderator/reflector and because this depends on the number of carbon atoms per $cm^3$, the density is of importance.
- the graphite needs to provide structural support to the fuel and coolant passages and thus, the mechanical strength is of importance.
- the graphite must be resistant to corrosion due to the coolant gas and impurities, but any corrosion and its effect on material properties needs to be accounted for.
- the graphite has to be dimensionally stable during fast neutron irradiation and any changes understood.

When assessing these functions and evaluating the lifetime of a graphite component, whether it is based on stress or strength based criteria[7], properties that need to be considered (in no particular order) are:

- Young's modulus
- Poisson's ratio
- thermal conductivity
- coefficient of thermal expansion (CTE)
- dimensional changes
- irradiation creep
- tensile strength
- compressive strength
- flexural strength
- fracture toughness

As can be seen, the list includes the majority of the material properties. Therefore, another criterion was applied.

## 2.2 Availability of data

In order to adequately create and validate any model it is essential that there are data available. A cursory examination of what data is and will be available has been conducted (Tables 2 & 3). With respect to the historical data, no attempt has been made to identify the actual details of the data. Only judgements as to the approximate quantity (with respect to each other property) and if the data encompassed the operating environment of a VHTR (dose, oxidation and temperature ranges) were made. Similar judgements were made with regards to the planned and ongoing measurements. Two significant features of the historical data were that the data does not cover the dose range envisaged (at the temperatures of interest). In fact there were little data for many of the properties.

Generally, the data referred to will have been irradiated in an inert atmosphere. To the author's knowledge there have been no experiments to examine the effect of combined irradiation and radiolytic oxidation on the material properties of graphite within the VHTR temperature range. Thus, it may be difficult to encompass and validate the radiolytic oxidation process within the model. This may not be of significance as the slow rate of oxidation may have negligible effect on the material properties. When each property is being examined for modelling, a judgement will be made as to the likely consequence of oxidation on the property. If it is deemed to be negligible in comparison with the irradiation effects, oxidation will be ignored. However, if oxidation is expected to have a significant effect, the possibility of including oxidation will have to be considered.

By using the amount of data available and to be available, it was possible to order the properties according to those with the most data:

- Dimensional change
- Thermal conductivity
- Young's modulus
- Thermal expansion
- Density
- Irradiation creep
- Strength
- Poisson's ratio
- Fracture toughness

**Table 2 Unirradiated graphite material properties measurements.**

| Property† | Quantity of data | |
|---|---|---|
| | Historical | Ongoing/planned |
| Young's modulus | high | high |
| Poisson's ratio | low | low/none |
| Strength | low | low |
| Fracture toughness | low | low/none |
| Thermal conductivity | high | high |
| CTE | high | high |
| Density | high | high |

†Dimensional change and irradiation creep are not applicable.

**Table 3 Irradiated graphite material properties measurements (T = temperature, D = dose, O=oxidation).**

| Property | Historical | | | | Ongoing/planned | | | |
|---|---|---|---|---|---|---|---|---|
| | Qty. | T† | D‡ | O | Qty. | T† | D‡ | O |
| Dimensional change | high | ✓ | × | × | high | ✓ | ✓ | × |
| Irradiation creep | low | ✓ | × | × | low | ✓ | × | × |
| Young's modulus | med | ✓ | × | × | high | ✓ | ✓ | × |
| Poisson's ratio | low | × | × | × | low/none | × | × | × |
| Strength | low | × | × | × | none | × | × | × |
| Fracture toughness | low | × | × | × | none | × | × | × |
| Thermal conductivity | high | ✓ | × | × | high | ✓ | ✓ | × |
| CTE | med | ✓ | × | × | high | ✓ | ✓ | × |
| Density | med | ✓ | × | × | high | ✓ | ✓ | × |

†Graphite temperatures of interest for a VHTR are 650-950°C.
‡Assumed maximum dose for a graphite component is ~25 dpa carbon (~190 × $10^{20}$ n/cm$^2$ EDN).

## 2.3 Current understanding of mechanisms

Another factor that was considered in the selection process was the level of understanding in the mechanisms behind the graphite property changes and the scale of these mechanisms (Table 4). A number of the properties (dimensional change, Young's modulus, thermal expansion, and density) have reasonable amounts of understanding or agreed theories as to the mechanisms that control the irradiation behaviour. The other properties have either unknown or disputed mechanisms, with some of the proposed mechanisms being of a nano- or atomistic scale.

**Table 4 Microstructural mechanisms behind material property changes in irradiated graphite.**

| Property | Agreement | Proposed mechanism/s | Scale |
|---|---|---|---|
| Dimensional change | ✓ | crystallite behaviour, porosity closure/formation | micro/nano |
| Thermal conductivity | × | phonon scattering, crystallite behaviour, crystallite boundaries, lattice defects | nano/micro |
| Young's modulus | | | |
| pinning | × | dislocations, crystallite elastic moduli | nano |
| structure | ✓ | porosity closure/formation | micro/nano |
| CTE | × | crystallite behaviour, structural rearrangement, porosity formation/closure | micro |
| Density | ✓ | crystallite behaviour, porosity closure/formation | micro |
| Irradiation creep | × | pinning/unpinning of dislocations, basal slip, structure changes | nano |
| Strength | × | Griffith theory, plasticity, crack generation, critical strain, critical stress, critical strain energy, density, Weibull, fracture mechanics | micro |
| Poisson's ratio | × | crystallite elastic moduli & Poisson's ratio, porosity formation/closure | nano/micro |
| Fracture toughness | × | crack bridging, crack tortuosity, process zone, localised stress intensification, porosity closure/formation | micro |

If the current understanding of the mechanisms behind the dimensional and property changes was the only criterion, the properties which have agreed or understood microstructural mechanisms be assessed first, followed by those with disputed microstructural mechanism, and finally by those with nano/atomistic mechanisms. However, when considering all of the criteria, the proposed order in which to examine the properties is:

- Dimensional change
- Young's modulus
- CTE
- Density
- Thermal conductivity
- Irradiation creep
- Strength
- Fracture toughness
- Poisson's ratio

# 3 Literature survey of modelling techniques (Task 4.2)

There are a number of modelling methods that use microstructural mechanics to determine the response of a heterogeneous material from the behaviour and arrangement of the constituents. The modelling techniques can generally be categorised depending upon how the microstructure is represented. These are summarised below, after which possible models for the properties highlighted in §2 are discussed in more detail.

## 3.1 Reproduction approach

This approach uses the finite element method (FEM) and is the easiest method to relate material behaviour with microstructural changes as it creates a direct representation of the microstructure (Figure 3). In a simple microstructure this may be relatively straightforward but as the microstructure becomes more complex, creating a model that is able to represent the phases and orientations of the constituents becomes more demanding. This not only makes the meshing procedure more complex and time consuming, but also makes the analysis more computationally expensive.

The meshing can be simplified using the multiphase element technique[9] where a regular mesh is superimposed on to the actual microstructure. The property associated with the colour of the underlying image is then assigned to the integration points of the elements. However, this technique can give a poor representation of the interfaces as some quantities that jump the interfaces can not be described adequately if the interface passes through the element[9]. Other variations of this technique are object-oriented finite element method (OOF)[10] and the extended finite element method (X-FEM)[11].

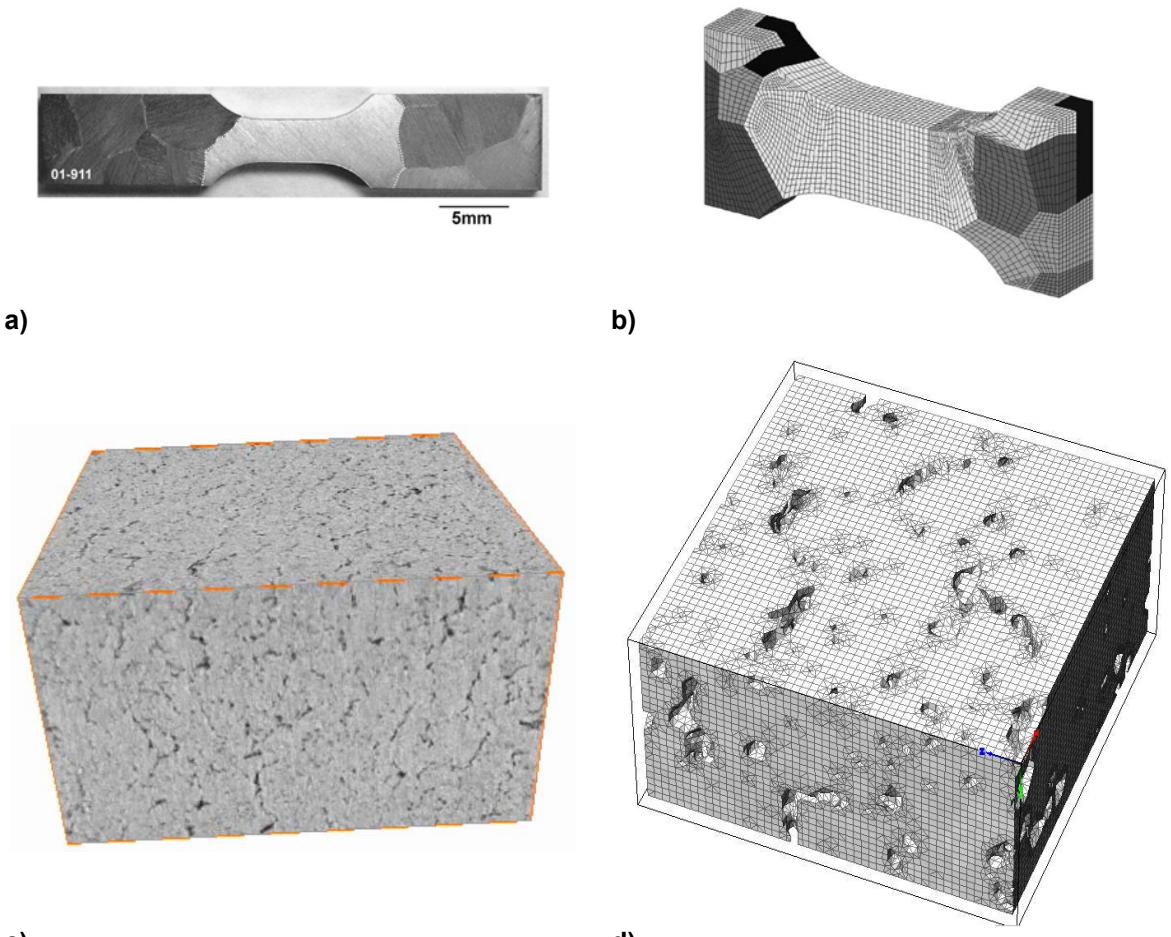


**Figure 3 Examples of the reproduction approach; a) micrograph of a tensile test specimen and b) respective finite element model[8]; c) X-ray tomography image of a graphite sample and d) respective finite element model (courtesy of C. Berre).**

## 3.2 Mean field approach

The mean field approach is a technique where localised fields (stress, strains etc.) within each constituent are approximated by the average of the phases. There are numerous ways of approximating the average, with some being of higher complexity, but generally the approximations are phase stress and phase tensors as these have small computational requirements[12].

This method usually does not explicitly account for the microstructure, although recent developments have included differences in porosity morphology and orientation[13]. It has also been demonstrated that some mean field methods may only be applicable in certain load conditions[14].

## 3.3 Unit cell method

The periodic microfield or unit cell method approximates a heterogeneous material using spatially periodic phase arrangements that can be simple or complex (Figure 4). If the microstructure is explicitly modelled, the initiation of damage at this level can be examined, but because of their periodic nature, the damage would be periodic. Thus, unit cells are not suitable for studying the interaction between microstructure and macroscopic cracking. A more general disadvantage is that the unit cells can be difficult to create and can be computationally expensive.

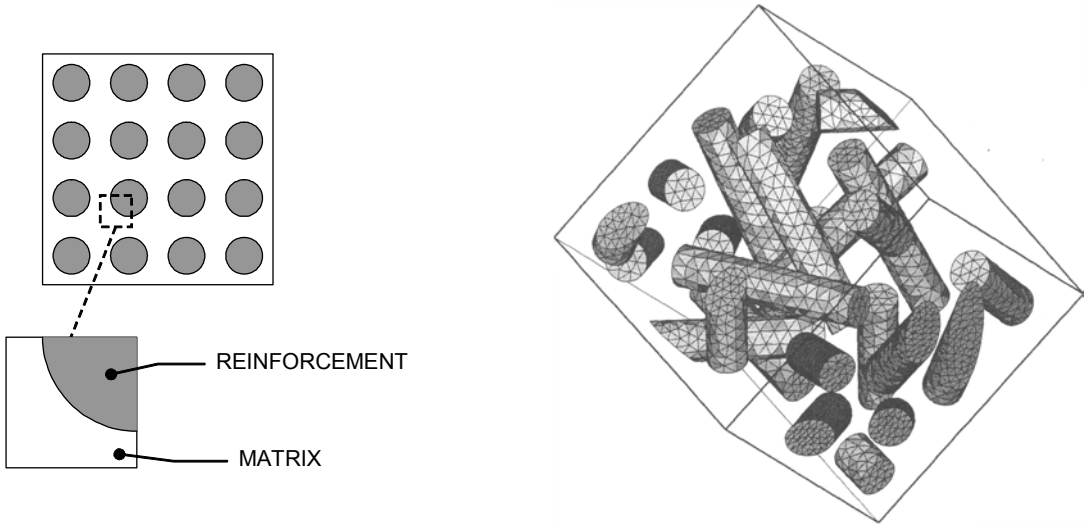


**Figure 4 Examples of unit cell models; a) 2D continuously reinforced composite; b) 3D short-fibre reinforced composite[12].**

Most unit cell models use standard finite element analyses, but there are special hybrids that apply analytical theories. One such example is the Voronoi finite element method (VCFEM)[15] where an equivalent microstructure is generated using the Dirichlet tessellation or Voronoi diagram. This technique uses a nearest-neighbour rule to create partitions, and when the Voronoi cell is completed, only a small number of Voronoi cells are required for analysis. Although these cells can be complex (Figure 5), it is reported that good computational efficiency and accuracy can be achieved[12].

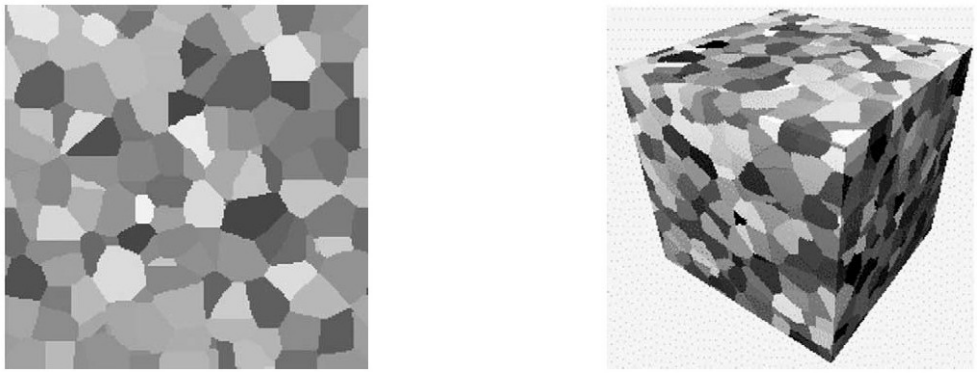

a) b)

**Figure 5 Examples of Voronoi cell models; a) 2D; b) 3D[9].**

## 3.4 Hierarchical approach

A development of the unit cell approach is the hierarchical method where the heterogeneous material is approximated using not a single unit cell but a range of unit cells (Figure 6). In the actual material, there are non-uniformities at global and local levels. This complexity and high computational requirements can be reduced by assuming uniformity at local levels and using different local cell models. The non-uniform global model can then be constructed from these local cell models. A disadvantage with this is that the creation and analysis of a range of local models can be time consuming.

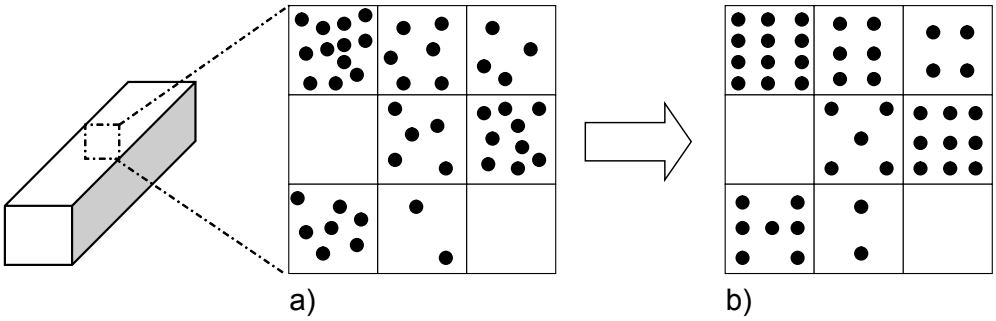

a) b)

**Figure 6 Hierarchical approach; a) globally and locally non-uniform; b) globally non-uniform but locally uniform[16].**

## 3.5 Embedded cell approach

The embedded cell method uses a discrete model of the microstructure, similar to a unit cell, surrounded by an approximation of the bulk material, the properties of which are determined from constitutive laws (Figure 7). The loads and displacements are

applied away from the discrete core region. This technique can be computationally expensive[12] but can be used to examine areas of particular interest such as crack tips and inclusions.

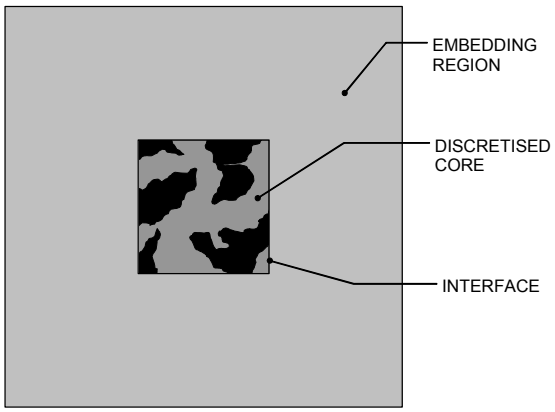


**Figure 7 Example of an embedded cell model.**

**Table 5 Advantages and disadvantages of the categories of mechanistic modelling.**

| Method | Advantages | Disadvantages |
|---|---|---|
| Reproduction | • uses actual microstructure | • complex model creation<br>• computationally expensive |
| Mean field | • low computational requirements | • possibly load case dependent<br>• does not explicitly model microstructure |
| Unit cell | • microstructure can be explicitly modelled in periodic structures<br>• computationally efficient | • periodic nature means an equivalent microstructure has to be used for inhomogeneous materials |
| Hierarchical | • quasi-periodic reduces computational requirements | • extensive numbers of models may have to be analysed |
| Embedded cell | • actual structure can be modelled | • can be computationally expensive<br>• requires constitutive equations |

## 3.6 Dimensional change

The changes in dimensions of a material when subjected to fast neutron irradiation occurs in a range of materials such as steels, SiC/SiC composites, and of course graphite. The majority of dimensional change modelling studies have been within the graphite field, but other materials have been examined. These examinations have generally been in the void swelling in effective mediums that are then used in data fitting in order to obtain analytical model parameters.

Many of the existing graphite dimensional change models are based upon a semi-empirical relationship[17] that related dimensional change with thermal expansion in irradiated graphite. Although the model included a "structure factor", it did not account for the actual structure of the graphite under examination. The relationship was also shown to diverge at higher doses. Later developments of this relationship[18, 19, 20, 21] proclaimed to include other microstructural features such as porosity generation but all used empirical relationships and had little, if any, microstructural basis.

A hierarchical/embedded cell approach has been used to obtain qualitative and quantitative dimensional change results for UK graphite grades[22] and a Russian graphite grade[23]. The technique involved using the finite element method to analyse the irradiation behaviour of graphite filler particles with various porosity volumes and morphologies, surrounded by an effective medium representing the binder phase (Figure 8). The filler behaviours were then implemented into a mesoscale model that represented the polycrystalline material (Figure 8). The distribution and arrangement of the filler results were based on to the composition of the graphite grade in question. At lower temperatures (450-600°C) the results compared well to experimental data, but at higher temperatures (900°C and above) the results did not compare as well. The original application was only in 2D and it was recommended that to fully account for the actual graphite structure and interactions, the model would have to be extended into 3D. The model also did not account for the effect of oxidation although it was postulated that this could be included.

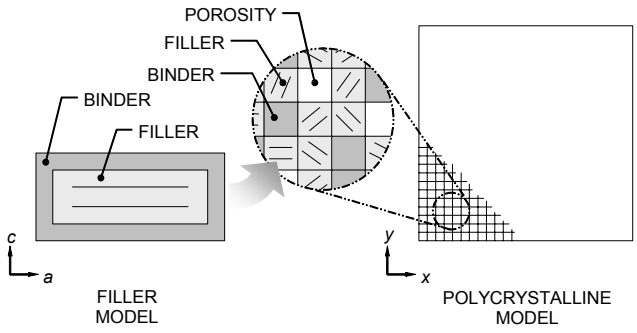


**Figure 8 Hierarchical/embedded cell approach used to model dimensional changes in nuclear grade graphite[22, 23].**

Other approaches may be suitable for modelling dimensional changes but as they have never been applied to this particular case, the development could be greater. The reproduction technique could be used in conjunction with the 3D X-ray tomography images. However, this would require the use of meshing software (such as Simpleware). The resolution of the X-ray tomography images would be important as it has been shown[22] that it is the smaller scale porosity that is important for the dimensional changes. It is probable that any such model would be computationally expensive. A mean field approach could be applied although it is anticipated that a multi-stage homogenisation process[13] would have to be used to encompass all of the microstructural features. This would increase the computation but it would still be the least computationally demanding method. A Voronoi FEM may not be applicable as an approach on its own as the discrete microstructure (the small scale porosity) would not be modelled. However, it may be useful in a hierarchical approach as the mesoscale model as it could provide a more representative structure in comparison to the square/cubic arrangement used previously[22, 23].

The two methods that are expected to be the most suitable for modelling dimensional changes are the hierarchical/embedded cell approach and the reproduction approach. The main reason for the first choice was that the technique has been successfully applied already to modelling dimensional changes at lower temperatures. The reproduction has been chosen as if it is successful, the ability to use x-ray tomography images of a graphite grade to directly predict the irradiation and oxidation behaviour would be extremely beneficial. The envisaged data and development requirements for the two chosen techniques are given below (Table 6). It should be noted that it has been assumed that for each property, measurements of the respective property at various irradiation and oxidation levels will be required for validation.

**Table 6 Candidate methods for modelling dimensional changes in nuclear grade graphites.**

| Method | Input data | Required developments |
|---|---|---|
| Hierarchical/ embedded | • embedding material properties<br>• graphite crystal properties<br>• crystallite orientations<br>• constituent ratios<br>• porosity distribution<br>• porosity morphology<br>• filler distribution | • 3D<br>• high temperature<br>• combined irradiation and oxidation |
| Reproduction | • graphite crystal properties<br>• crystallite orientations<br>• constituent ratios | • irradiation<br>• combined irradiation and oxidation |

## 3.7 Young's modulus

The use of microstructural modelling to predict Young's modulus has been applied to porous materials and often these have been semi-empirical and predict only the effect of porosity volume changes. A hierarchical or multilevel superelement technique was applied to determine the effective elastic properties of a porous material[24]. Such approaches have been used for the effect of oxidation only and thus, may have some use in part of a Young's modulus model. Nevertheless, the irradiation induced changes may be caused by more than just changes in porosity.

The current prediction methods for graphite Young's modulus use an empirical relationship that divides the changes into two terms; pinning and structure. Pinning is said to saturate at low doses and to be due to atomic/nanoscale changes. Thus, pinning is not going to be considered here as it is below the microstructural scale. The structure term accounts for changes in the microstructure and can be considered here. The only microstructural model to have been applied to the Young's modulus of irradiated graphite was that also used for the dimensional changes[22, 23]. The results were qualitative but did not wholly correspond to experiment, especially at high temperatures. As with the dimensional change model, the model was only in two-dimensions and did not include oxidation effects.

An investigation[25] is currently underway to examine the use of X-ray tomography images in predicting the Young's modulus of graphite with different amounts of porosity. Initial results are promising and such a reproduction technique may be developed to account for irradiation, although the question of resolution and the small scale porosity is still applicable.

As the Young's modulus is postulated to be related to the dimensional changes, it should be possible to model both of the behaviours with the same model or procedure, as demonstrated in the hierarchical/embedded cell approach[22, 23]. Hence, the approaches chosen are those for dimensional changes i.e. hierarchical/embedded cell and reproduction approach (Table 7).

**Table 7 Candidate methods for modelling Young's modulus in nuclear grade graphites.**

| Method | Input data | Required developments |
|---|---|---|
| Hierarchical/ embedded | • embedding material properties<br>• graphite crystal properties<br>• crystallite orientations<br>• constituent ratios<br>• porosity distribution<br>• porosity morphology<br>• filler distribution | • 3D<br>• high temperature<br>• combined irradiation and oxidation |
| Reproduction | • graphite crystal<br>• crystallite orientations<br>• constituent ratios | • irradiation<br>• combined irradiation and oxidation |

## 3.8 Coefficient of thermal expansion

The Voronoi cell method has been used to calculate the effective thermal expansion coefficient of a fully-dense (no porosity) polycrystalline material from single crystal thermo-elastic properties and polycrystalline elastic properties[26]. The results were found to be close to experimental and theoretical results and although it was not encompassed within the study, it may be possible to include porosity within this type of model. However, this may not lend it to modelling irradiation induced changes due to the size range of the porosity.

In the graphite field, the majority of the thermal expansion work has been on semi-empirical relationships between unirradiated crystallite CTE and polycrystalline CTE[27, 28] that had little microstructural basis. A novel approach to model both the irradiation and oxidation changes in the CTE of a UK graphite grade was developed by Hacker[29]. In this technique, a two-dimensional array of so-called spherical single crystals (SSCs) was constructed (Figure 9). The different levels of porosity were represented using SSCs of different sizes and with different numbers of layers; the size distribution being calculated from analyses of micrographic images. An algorithm was applied to pack the SSCs into a "box" and to transmit the individual SSC changes to the bulk. The effects of irradiation and oxidation where then applied to the individual SSCs and the overall response calculated (Figure 9). The model results compared well with experimental data, although at high oxidation levels the results diverged (said to be caused by the percolation limit of the model). The model did use some microstructural information (particle size distribution) it is unknown if the technique would be applicable to other graphite grades as the UK grade examined was Gilsocarbon, a graphite with spherical filler particles. There are also concerns as to the development of the model into three-dimensions.

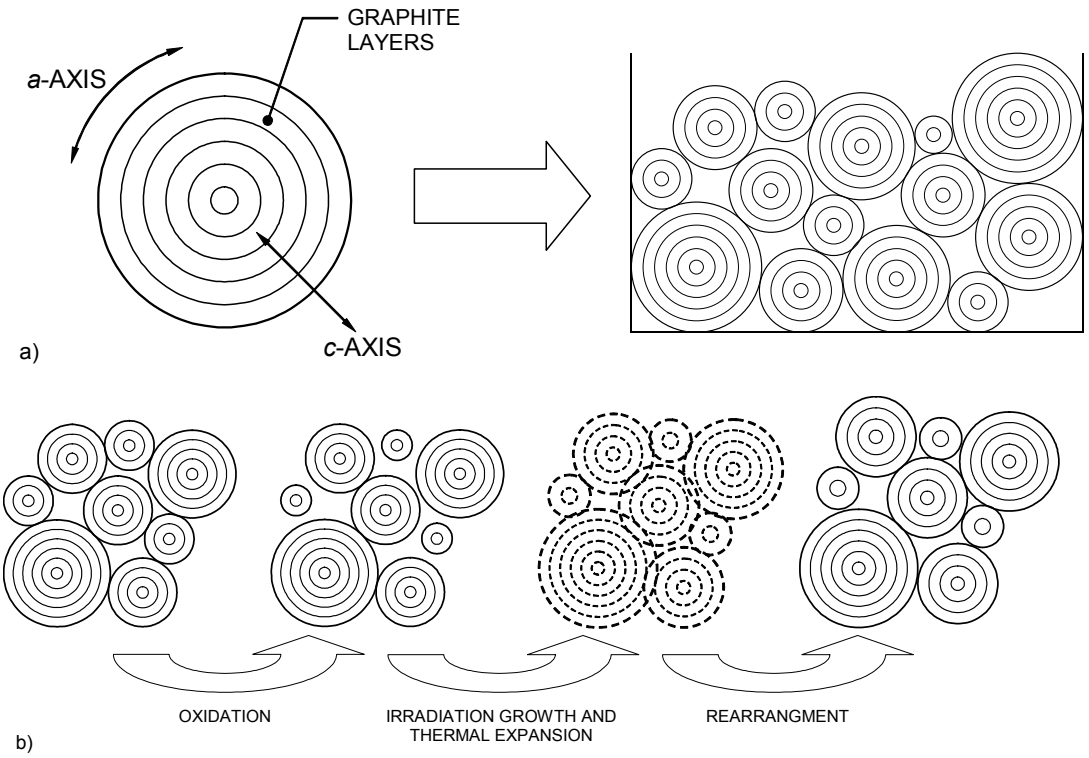


**Figure 9 Hacker approach[29] used to model CTE of nuclear grade graphite; a) an SSC and packing in a "box"; b) analysis sequence.**

The hierarchical/embedded cell concept was unsuccessfully applied to irradiated graphite CTE[22] with the reason for its failure being attributed to the inability of the model to account for the smaller scale changes associated with CTE. However, the inability of the model to predict CTE may have been more a result of the inadequacy of the boundary conditions and the fact that the model was in 2D.

It is suggested that because the hierarchical/embedded cell and reproduction techniques are the prime candidates for dimensional changes and Young's modulus, that these should be initially applied to the changes in CTE. There is also evidence that the Voronoi cell method, which could be part of the hierarchical/embedded cell technique, is suitable for modelling the CTE. If preliminary results do not demonstrate the possibility of modelling the CTE changes, the Hacker approach shall be investigated.

**Table 8 Candidate methods for modelling CTE in nuclear grade graphites.**

| Method | Input data | Required developments |
|---|---|---|
| Hierarchical/ embedded | • embedding material properties<br>• graphite crystal properties<br>• crystallite orientations<br>• constituent ratios<br>• porosity distribution<br>• porosity morphology<br>• filler distribution | • 3D<br>• high temperature<br>• combined irradiation and oxidation |
| Reproduction | • graphite crystal properties<br>• crystallite orientations<br>• constituent ratios | • irradiation<br>• combined irradiation and oxidation |
| Hacker | • filler particle size distribution<br>• porosity distribution<br>• graphite crystal CTE | • 3D |

## 3.9 Density

There is very little work on the microstructural modelling of densification of graphite or any other material. One study[30] did use the Voronoi cell method to model the densification of a cemented carbide during the sintering process. The 2D finite element model included tungsten carbide particles embedded in a cobalt matrix, with there also being a range of large pores. By using a “sintering stress” (surface energy at the pores) the results of a simulated densification process were shown to be comparable with experimental data.

A similar procedure may be suitable for the case of irradiated and oxidised graphite. In this case, the driving force would be the filler particle behaviour that causes the closure and opening of porosity (dimensional changes, CTE and Young’s modulus). This may require a hierarchical approach to obtain the local behaviour but this could then be implemented in a Voronoi cell model that represents the mesoscale structure. The model would also have to be extended into three dimensions. As the reproduction method will also be used to evaluate dimensional changes, CTE and Young’s modulus, it is proposed that this method be examined for modelling the density changes.

**Table 9 Candidate methods for modelling density in nuclear grade graphites.**

| Method | Input data | Required developments |
|---|---|---|
| Hierarchical /embedded | • embedding material properties<br>• graphite crystal properties<br>• crystallite orientations<br>• constituent ratios<br>• porosity distribution<br>• porosity morphology<br>• filler distribution | • 3D<br>• high temperature<br>• combined irradiation and oxidation |
| Reproduction | • graphite crystal properties<br>• crystallite orientations<br>• constituent ratios | • irradiation<br>• combined irradiation and oxidation |

## 3.10 Thermal conductivity

Microstructural modelling has been used to calculate the thermal conductivities of numerous materials. The unit cell approach has been applied extensively to composites with periodic structures, and in one particular study[31] the model included sub-models that represented manufacturing porosities identified through SEM (scanning electron microscopy) analyses. The thermal conductivity of a porous ceramic has been determined using a reproduction method[32]. The 2D finite element model consisted of two phases (a solid phase and a porous phase) the arrangement of which were obtained from micrographs of the material. The results compared well with analytical results at lower pore volumes (<20%) but diverged at higher porosity volumes. This was attributed to a percolation limit in the 2D model which was said to be resolved if the model was extended to 3D. An artificial neural network (ANN) and Voronoi cell combination technique has also been used to model the effective thermal conductivity of an unidirectional composite[33]. This approach included information on each phase such as matrix and reinforcement conductivities, fibre volume fraction, and geometrical arrangements. As the spatial arrangement of the fibres or microstructure was not uniform, a 2D Voronoi tessellation was used to quantify the structure. Different regression models were considered and the results compared with effective thermal conductivity calculated using the finite element method. The main advantage of this technique over the finite element method was that the computation time was significantly less, although the ANN required “training”.

A hierarchical approach has been employed to simulate the thermal conductivity of porous cometary ice[34]. The structure was an aggregate of grains with a size distribution over several orders of magnitude, and a similar distribution of pores. A random and fractal porous structure was assumed and a 3D Monte Carlo model used. The model consisted of two units, filled and void, randomly distributed according to a predetermined porosity volume (Figure 10). The effective thermal conductivity for the

basic cube was solved and used as a filled unit cell in a larger cube, building up the hierarchical structure. In this way an effective thermal conductivity for the material was determined. At porosities greater than 70%, the percolation limit was reached. The model was not compared with any experimental results but it was stated that the model should be applicable to realistic configurations, although it may not pertinent to materials with a normal distribution of pore sizes (only power law pore size distribution close to 3).

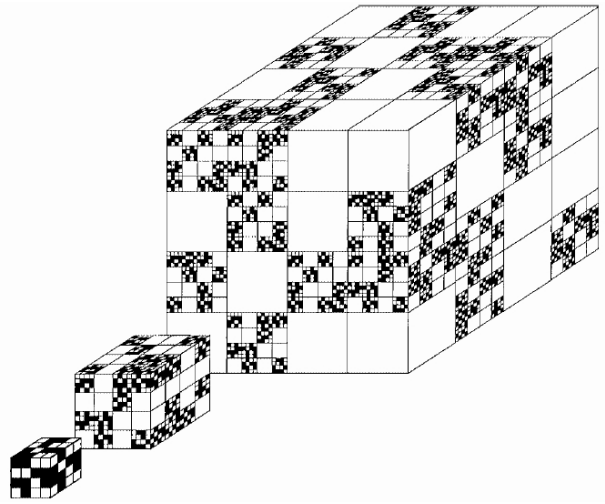

**Figure 10 Hierarchical approach used to model the thermal conductivity of cometary ice[34].**

In the graphite research field, thermal conductivity has usually been predicted using empirically based relationships between polycrystalline and crystalline thermal conductivities. The effective thermal conductivity of graphite has been modelled by representing the material as a series of links and junctions[35]. This analytical model required knowledge of the principal conductivities ratio, conductivity along the graphite basal plane, density and microstructural features such as crystallite size and shape. Good agreement was found between the predictions and experimental data for unirradiated graphite. If the relevant input data can be obtained for irradiated and oxidised graphite, it may be possible to use such a model.

Another analytical technique that uses data from X-ray tomography images has also been developed[36]. By classifying the porosity network in thermally oxidised samples in terms of shape of isolated pores and fractions of isolated/continuous porosity, a Euler based approach was shown to have good agreement with experimental data. If the thermal conductivity of irradiated and oxidised graphite is still a function of the model's inputs (crystallite thermal conductivities, and porosity morphology and distribution) it may be possible to extend this procedure to encompass these changes.

The most promising technique is perceived to be the analytical Euler-based method[36] as this has already been shown to be applicable to oxidised graphite and uses data

that should be readily available. As the hierarchical method has been used for thermal conductivity of another material and has been selected for another property, it is proposed that the hierarchical also be examined. The reproduction will also be examined for this property as it is being developed for other properties.

**Table 10 Candidate methods for modelling thermal conductivity in nuclear grade graphites.**

| Method | Input data | Required developments |
|---|---|---|
| Analytical Euler-based | • graphite crystal thermal conductivity<br>• porosity morphology and distribution | • radiolytic oxidation<br>• irradiation |
| Hierarchical /embedded | • embedding material properties<br>• graphite crystal properties<br>• crystallite orientations<br>• constituent ratios<br>• porosity distribution<br>• porosity morphology<br>• filler distribution | • 3D<br>• high temperature<br>• combined irradiation and oxidation |
| Reproduction | • graphite crystal properties<br>• crystallite orientations<br>• constituent ratios | • irradiation<br>• combined irradiation and oxidation |

## 3.11 Irradiation creep

Most relationships for creep, whether it be thermal or irradiation creep, are based upon empirical fits that have little, if any, representation of the structure within the material. Of the studies that do examine the microstructure while it is under creep, many focus upon the formation of damage caused by creep[37, 38] and not the evaluation of a creep law or relationship. There have been however, some examinations into using microcrack descriptions and damage mechanics to determine the creep behaviour of polycrystalline materials. One such study[39] used a 3D creep damage model that assumed parallel flat microcracks. By employing a damage vector that could simultaneously describe different damage processes, theoretical results that were comparable to experimental data were obtained. However, the model required data from 3 empirical functions obtained from experiments. A similar study into the creep of rock salt[40] used so-called multi-mechanism deformation (MD) and multi-mechanism deformation coupled fracture (MDCF) models. The assumption was that both dislocation slip and creep damage in the form of microcracks contributed to the macroscopic creep. The results compared well with experimental data but again there was a requirement to determine “material constants” through experiments.

The relationships in the irradiated graphite area have also tended to be empirically or semi-empirically based. Very little work has been done in microstructurally modelling the creep behaviour. Possible reasons for this is the lack of agreement in the mechanisms behind irradiation creep, and the difficulties and high costs associated with conducting irradiation creep experiments.

Although none of the approaches currently provide a means to predict irradiation creep from data on graphite microstructure (they require empirical fits), it is suggested that the microcrack damage model and MD/MDCF model be applied with the aim to remove the reliance upon empirical data through the use of other microstructural models or information.

**Table 11 Candidate methods for modelling irradiation creep in nuclear grade graphites.**

| Method | Input data | Required developments |
|---|---|---|
| Microcrack damage | • creep damage functions | • remove empirical data<br>• irradiation<br>• oxidation |
| MD/MDCF | • elastic properties<br>• 17 material constants | • remove empirical data<br>• irradiation<br>• oxidation |

## 3.12 Strength

The strength or failure of brittle materials have classically been assessed in numerous ways including the Griffith theory, Weibull theory, critical strain energy density criterion, critical stress criterion, critical strain criterion, and linear elastic fracture mechanics (LEFM). However, there approaches ignore microstructural features to a greater or lesser extent. Object oriented finite element (OOF) analyses have been combined with the Griffith theory to examine porous glass[41] and tungsten carbide cobalt[42]. The obtained results were comparable to experimental data but both models were two-dimensional, the glass model was a homogeneous material with porosity, and the tungsten carbide cobalt used an empirical factor. A different approach has been used in the study of fracture in concrete[43, 44]. In this study the concrete was represented by a lattice network of particles connected by springs, and granular mechanics was used to treat the network as an equivalent continuum. A maximum strength failure criterion was applied to the beams and fracture behaviour comparable to experimental results was achieved. However, the model was again 2D and did not include explicit microstructural information. A 3D model based on the domain of microcrack growth (DMG) concept was used to simulate quasi-brittle solids under tension[45]. This approach used a representative volume element (RVE) with a density of randomly distributed penny-shaped cracks. The study gave qualitative

results but the model assumed that the material was statistically homogeneous and the that the concentration of microcracks was not large.

The statistically based approaches such as Griffith and Weibull have dominated the graphite research field and, as well as not including explicit microstructural information, they have been shown to be inappropriate when applied independently[46, 47, 48]. A model developed by Burchell[49] combined a fracture mechanics failure criteria with a microstructurally based description of fracture to give quantitative unirradiated and qualitative irradiated results. The model used a cubic array of randomly oriented grains and pores, with each grain assumed to contain a plane of weakness (a cleavage plane) oriented to some angle (Figure 11). The grains had a mean filler particle size, and the pores were randomly positioned and had a log-normal size distribution according to microstructural information. Using linear elastic fracture mechanics (LEFM), cracks were said to initiate from the pores and propagate by fracture along the cleavage planes. A development of the Burchell model[50] was said to give better results in some cases but it required greater amounts of input data that included non-microstructural and iterative data.

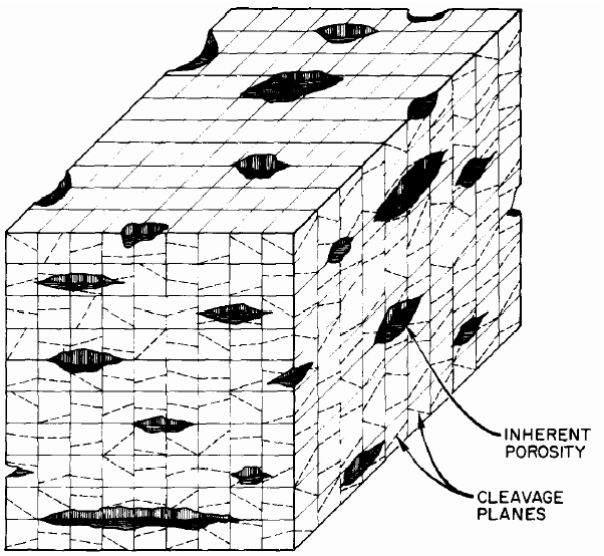


**Figure 11 Burchell model[49] used for the fracture and strength of nuclear grade graphites.**

A different concept that has been used for graphite fracture was the continuum damage mechanics (CDM) model[51]. In this, both stress-based and fracture mechanics based failure criteria were included in a 2D finite element mesh. Damage initiation was controlled by the stress criterion whilst the formation of the crack was controlled by the fracture mechanics criterion. Good agreement with experimental data was found, but the method did not account for microstructure and required that the crack path be predetermined. This could be obtained by combining the CDM with the reproduction approach.

The proposed approach is the Burchell model as it uses microstructural features and has been applied, with varying levels of success, to unirradiated and irradiated graphite. The second choice is the CDM model with the requisites that it be implemented in three-dimensions and include microstructural features.

**Table 12 Candidate methods for modelling strength in nuclear grade graphites.**

| Method | Input data | Required developments |
|---|---|---|
| Burchell model | • mean filler size<br>• bulk density<br>• mean pore size<br>• pore distribution<br>• porosity volume<br>• specimen volume<br>• fracture toughness (grain) | • irradiation<br>• oxidation |
| CDM/ reproduction | • bulk elastic properties<br>• energy release rate | • 3D<br>• microstructure link<br>• irradiation<br>• oxidation |

## 3.13 Fracture toughness

The majority of examinations into the modelling of the fracture toughness (or stress intensity factor) have not predicted the fracture toughness directly but have investigated the proposed mechanisms and the effect of their change on the fracture toughness value i.e. parametric studies with fracture toughness quoted as normalised values[52, 53, 54]. When an actual fracture toughness value was given, some degree of calibration of fitting has been used to give values that were comparable to experimental data[55, 56, 57]. A study[58] that did compute the fracture toughness for steel directly used quantum physics and continuum mechanics to calculate the value from first principles. This type of computation is deemed to be beyond the scope of this work.

The author was unable to find any investigations into the microstructural modelling of graphite fracture toughness. The only graphite/carbon study was that for a carbon foam[59] and this used a periodic cell arrangement to consider the variation of fracture toughness as a function of the solidity of the foam.

It is proposed there is at present no clear microstructural modelling approach to determining a fracture toughness value for graphite. It may however, be possible to use X-ray tomography and the reproduction approach to examine the formation of damage along and ahead of the crack, and its effect on the fracture toughness.

**Table 13 Candidate methods for modelling change fracture toughness in nuclear grade graphites.**

| Method | Input data | Required developments |
|---|---|---|
| Reproduction | • graphite crystal properties<br>• crystallite orientations<br>• constituent ratios | • irradiation<br>• combined irradiation and oxidation |

## 3.14 Poisson's ratio

Although specific studies into the Poisson's ratio of a material have been conducted, these have usually been on materials with unusual Poisson's ratios i.e. negative Poisson's ratios[60]. Most examinations of a material's Poisson's ratio have been included as part of an investigation into the elastic properties. Thus, this property will be included in the modelling of the graphite Young's modulus (§3.7).

**Table 14 Candidate methods for modelling Poisson's ratio in nuclear grade graphites.**

| Method | Input data | Required developments |
|---|---|---|
| Hierarchical /embedded | • embedding material properties<br>• graphite crystal properties<br>• crystallite orientations<br>• constituent ratios<br>• porosity distribution<br>• porosity morphology<br>• filler distribution | • 3D<br>• high temperature<br>• combined irradiation and oxidation |
| Reproduction | • graphite crystal properties<br>• crystallite orientations<br>• constituent ratios | • irradiation<br>• combined irradiation and oxidation |

## 3.15 Input data

A recurring requirement of many of the models is that the behaviour of graphite constituents are required as input data. This will often be in the form of data from crystallite graphite i.e. irradiation and oxidation behaviour of graphite flakes or HOPG (highly oriented pyrolytic graphite). There is however, very little information on these materials, especially at higher doses and temperatures. Although some approximations can be made, this will ultimately reduce the accuracy and reliability of any models. The author therefore recommends that if microstructural models are to be used, obtaining comprehensive material property data on HOPG covering the operating conditions of VHTRs needs to be considered.

# 4 Conclusions

- The graphite material properties to be examined and the sequence in which to do this has been determined by considering the designers' and operators' requirements, availability of data, and current understanding of the mechanisms behind the property changes.

- The sequence in which to examine the properties is dimensional change, Young's modulus, coefficient of thermal expansion, density, thermal conductivity, irradiation creep, strength, fracture toughness, and Poisson's ratio.

- Numerous modelling approaches from both the graphite and general materials fields were examined and their applicability to the VHTR graphite case considered. For each property to be examined, at least 1 candidate technique was chosen, although usually 2 or 3 were shortlisted.

- Most of the approaches require constituent behaviour as an input. There is very little of this data available for the required environment (dose, temperature, and oxidation) which could restrict the effectiveness of any models. This shortfall needs to be addressed.

# 5 Future work

The work will continue as per the initial proposal plan[2] with the short term plan being to examine the candidate approaches in more detail and to select 2 graphite grades that will be examined using these approaches (Task 4.4). The techniques will then be applied and their ability, or possible ability, to predict graphite behaviour assessed (Task 4.5). From these initial predictions, the best approach for each approach will be identified (Task 4.6), developed further (Task 4.7), and then reapplied (Task 4.8). The whole modelling, development and predictions will then be reported (Task 4.9). Properties will be provisionally examined in sequence but when the properties use the same approach or model, more then one property may be examined.

# 6 References

[1] D. Buckthorpe. *Sub-project ML: Materials Development, SP-ML-WP3: Graphite Materials, Graphite Materials – Work plan for first 18 months*. 12820/TR/001 Issue 01, NNC Limited, 2005.
[2] G. Hall. *European Commission 6th Euratom Framework Programme 2002-2006, Sub-project ML: Materials Development, SP-ML-WP3: Graphite Materials, Task*

*4 programme*. NGRG P162 Issue 1, Nuclear Graphite Research Group, The University of Manchester, 2005.
[3] N. Baluc, W. Hoffelner, O. Gélineau, J. Linke, G. Korb, D. Buckthorpe, J. van der Laan and G. Brinkmann. *Material user requirement specification for very high temperature reactors (VHTRs)*. EXM-SP3-SPE-EPF-0002 Rev. g, ExtreMat IP, 2005.
[4] L. Salvo, P. Cloetens, E. Maire, S. Zabler, J.J. Blandin, J.Y. Buffière, W. Ludwig, E. Boller, D. Bellet and C. Josserond. *X-ray micro-tomography an attractive characterisation technique in materials science*. Nuclear Instruments and Methods in Physics Research B, 200, pp. 273-286, 2003.
[5] H. Nickel, H. Nabielek, G. Pott and A.W. Mehner. *Long time experience with the development of HTR fuel elements in Germany*. Nuclear Engineering and Design, 217, pp. 141-151, 2002.
[6] G. Haag, D. Mindermann, G. Wilhelmi, H. Persicke and W. Ulsamer. *Development of reactor graphite*. Journal of Nuclear Materials, 171, pp. 41-48, 1990.
[7] T. Oku and M. Ishihara. *Lifetime evaluation of graphite components for HTGRs*. Nuclear Engineering and Design, 227, pp. 209-217, 2004.
[8] R. John, W.J. Porter and S. Olson. *Measurement and modelling of orthotropic elastic behaviour of grains in a gamma titanium aluminide alloy*. Intermetallics, 12, pp. 1-9, 2004.
[9] G. Cailletaud, S. Forest, D. Jeulin, F. Feyel, I. Galliet, V. Mounoury and S. Quilici. *Some elements of microstructural mechanics*. Computational Materials Science, 27, pp. 351-374, 2003.
[10] N. Chawla, B.V. Patel, M. Koopman, K.K. Chawla, R. Saha, B.R. Patterson, E.R. Fuller and S.A. Langer. *Microstructure-based simulation of thermomechanical behaviour of composite materials by object-oriented finite element analysis*. Materials Characterization, 49, pp. 395-407, 2003.
[11] N. Moës, M. Cloirec, P. Cartraud and J.F. Remacle. *A computational approach to handle complex geometries*. Computer Methods in Applied Mechanics and Engineering, 192, pp. 3163-3177, 2003.
[12] H.J. Böhm. *A short introduction to selected chapters of numerical continuum micromechanics*. Frontiers of Computational Micromechnics in Industrial and Engineering Materials, European Advanced Summer School, The National University of Ireland, Galway, August 24$^{th}$ – 30$^{th}$, 2000.
[13] I. Doghri and L. Tinel. *Micromechanical modeling and computation of elasto-plastic materials reinforced with distributed-orientation fibers*. International Journal of Plasticity, 21, pp. 1919-1940, 2005.
[14] J. H. You, O. Poznansky and H. Bolt. *A comparative study on two elasto-plastic mean field methods*. Materials Science and Engineering, A344, pp. 201-208, 2003.
[15] S. Ghosh and R.L. Mallet. *Voronoi cell finite elements*. Computers and Structures, 50 (1), pp. 33-46, 1994.
[16] M. Geni and M. Kikuchi. *Damage analysis of aluminum matrix composite considering non-uniform distribution of SiC particles*. Acta Metallurgica, 46 (9), pp. 3125-3133, 1998.

[17] J.H.W. Simmons. *A relation between thermal expansion and dimensional change for polycrystalline graphite*. AERE-R3883, UKAEA Research Group Report, 1961.
[18] B.T. Kelly and J.E. Brocklehurst. *Dimensional changes of graphite at high fast neutron doses*. Proceedings of the Third Conference on Carbon, Buffalo, New York, pp. 172-175, 1972.
[19] J.E. Brocklehurst and B.T. Kelly. *Analysis of the dimensional changes and structural changes in polycrystalline graphite under fast neutron irradiation*. Carbon, 31 (1), pp. 155-178, 1993.
[20] G.B. Neighbour. *Modelling of dimensional changes in irradiated nuclear graphites*. Journal of Physics D: Applied Physics, 33, pp. 2966-2972, 2000.
[21] G. Hall, B.J. Marsden, S.L. Fok and J. Smart. *The relationship between irradiation induced dimensional change and the coefficient of thermal expansion: a modified Simmons relationship*. Nuclear Engineering and Design, 222, pp. 319-330, 2003.
[22] G. Hall. *Microstructural modelling of nuclear grade graphite*. EngD Thesis, The University of Manchester, 2004.
[23] B.J. Marsden, G. Hall and S.L. Fok. *Methods for the prediction of graphite irradiation dimensional and property changes in pressure tube reactor graphite*. Proceedings of an International Conference on Pressure Tube Reactors: Problems and Solutions, Moscow, October 19th – 22nd, 2004.
[24] J.P. Fan, C.Y. Tang and C.L. Chow. *A multilevel superelement technique for damage analysis*. International Journal of Damage Mechanics, 13, pp. 187-199, 2004.
[25] C. Berre, S.L. Fok and B.J. Marsden. *Establishing the relationships between microstructure and bulk mechanical properties of graphite*. NGRG R166 Issue 1, The University of Manchester, 2005.
[26] S. Kumar and S.K. Kurtz. *Simulation of material microstructure using a 3D Voronoi tessellation: calculation of effective thermal expansion coefficient of polycrystalline materials*. Acta Metallurgica et Materialia, 42 (12), pp. 3917-3927, 1994.
[27] A.L. Sutton and V.C. Howard. *The role of porosity in the accommodation of thermal expansion in graphite*. Journal of Nuclear Materials, 7 (1), pp. 58-71, 1962.
[28] G.M. Jenkins. *The thermal expansion of polycrystalline graphite*. Journal of Nuclear Materials, 13 (1), pp. 33-39, 1963.
[29] P.J. Hacker. *A study of the coefficient of thermal expansion of nuclear graphite*. PhD Thesis, University of Bath, 2001.
[30] L. Mähler and K. Runesson. *Modelling of solid-phase sintering of hardmetal using a mesomechanics approach*. Mechanics of Cohesive-Frictional Materials, 5, pp. 653-671, 2000.
[31] J.K. Farooqi and M.A. Sheikh. *Finite element modelling of thermal transport in ceramic matrix composites*. Computational Materials Science, article in press, 2005.
[32] S. Grandjean, J. Absi and D.S. Smith. *Numerical calculations of thermal conductivity if porous ceramics based on micrographs*. Journal of the European Ceramic Society, article in press, 2005.

[33] I. Turias, J.M. Gutiérrez and P. Galindo. *Modelling the effective thermal conductivity of an unidirectional composite by the use of artificial neural networks*. Composites Science and Technology, 65, 609-619, 2005.
[34] Y. Shoshany, D. Prialnik and M. Podolak. *Monte Carlo modeling of the thermal conductivity of porous cometary ice*. Icarus, 157, pp. 219-227, 2002.
[35] D.F. Pedraza and P.G. Klemens. *Effective conductivity of polycrystalline graphite*. Carbon, 31 (6), pp. 951-956, 1993.
[36] L. Babout, T.J. Marrow, P. Mummery and B.J. Marsden. *X-ray tomographic observations applied to porosity models for the thermal properties of oxidised nuclear graphite*. Conference on the Aging Management of Graphite Reactor Cores, The University of Cardiff, Wales, November 28th – 30th, 2005.
[37] N. Carrère, S. Kruch, A. Vassel and J.L. Chaboche. *Damage mechanisms in unidirectional SiC/Ti composites under transverse creep loading: experiments and modeling*. International Journal of Damage Mechanics, 11, pp. 41-63, 2002.
[38] T. Asayama and S. Hasebe. *Weld metal creep-fatigue life prediction by modeling the microstructure degradation due to the exposure to high temperature and load*. Nuclear Engineering and Design, 195, pp. 197-210, 2000.
[39] J. Betten, S. Sklepus and A. Zolochevsky. *A microcrack description of creep damage in crystalline solids with different behaviour in tension and compression*. International Journal of Damage Mechanics, 8, p. 197-232, 1999.
[40] K.S. Chan, S.R. Bodner, A.F. Fossum and D.E. Munson. *A damage mechanics treatment of creep failure in rock salt*. International Journal of Damage Mechanics, 6, pp. 121-152, 1997.
[41] V. Cannillo, C. Leonelli, T. Manfredini and M. Montorsi. *Computational simulations for the assessment of the mechanical properties of glass with controlled porosity*. Journal of Porous Materials, 10, pp. 189-200, 2003.
[42] C.S. Kim, T.R. Massa and G.S. Rohrer. *Modeling the relationship between microstructural features and the strength of WC-Co composites*. International Journal of Refractory Metals & Hard Materials, 24, pp. 89-100, 2006.
[43] C.S. Chang, T.K. Wang, L.J. Sluys, J.G.M. van Mier. *Fracture modeling using a micro-structural mechanics approach – I. Theory and formulation*. Engineering Fracture Mechanics, 69, pp. 1941-1958, 2002.
[44] C.S. Chang, T.K. Wang, L.J. Sluys, J.G.M. van Mier. *Fracture modeling using a micro-structural mechanics approach – II. Finite element analysis*. Engineering Fracture Mechanics, 69, pp. 1959-1976, 2002.
[45] X. Feng and D. Gross. *Three-dimensional micromechanical model for quasi-brittle solids with residual strains under tension*. International Journal of Damage Mechanics, 9, pp. 79-110, 2000.
[46] M.O. Tucker, A.P.G. Rose and T.D. Burchell. *The fracture of polygranular graphites*. Carbon, 24 (5), pp. 581-602, 1986.
[47] B.C. Mitchell, J. Smart, S.L. Fok and B.J. Marsden. *The mechanical testing of nuclear graphite*. Journal of Nuclear Materials, 322, pp. 126-137, 2003.
[48] J.E. Brocklehurst and M.I. Darby. *Concerning the fracture of graphite under different test conditions*. Materials Science and Engineering, 16, pp. 91-106, 1974.

[49] T.D. Burchell. *A microstructurally based fracture model for polygranular graphites*. Carbon, 34 (3), pp. 297-316, 1996.
[50] M.O. Tucker and N. McLachlan. *Fracture and microstructure of graphites*. Journal of Physics D: Applied Physics, 26, pp. 893-907, 1993.
[51] Z. Zou, S.L. Fok, S.O. Oyadiji and B.J. Marsden. *Failure predictions for nuclear graphite using a continuum damage mechanics model*. Journal of Nuclear Materials, 324, pp. 116-124, 2004.
[52] G. Liu, G.J. Zhang, X.D. Ding, J. Sun and K.H. Chen. *Dependence of fracture toughness on multiscale second phase particles in high strength Al alloys*. Materials Science and Technology, 19, pp. 886-896, 2003.
[53] B. Z. Margolin, A.G. Gulenko and V.A. Shvetsova. *Probabilistic model for fracture toughness prediction based on the new local fracture criteria*. International Journal of Pressure Vessels and Piping, 75, pp. 307-320, 1998.
[54] S.B. Biner. *A FEM analysis of crack growth in microcracking brittle solids*. Engineering Fracture Mechanics, 51 (4), pp. 555-573, 1995.
[55] Q.D. Yang, B.N. Cox, R.K. Nalla and R.O. Ritchie. *Fracture length scales in human cortical bone: the necessity of nonlinear fracture models*. Biomaterials, 27, pp. 2095-2113, 2006.
[56] J.H. Hanson and A.R. Ingraffea. *Using numerical simulations to compare the fracture toughness values for concrete from the size-effect, two-parameter and fictitious crack models*. Engineering Fracture Mechanics, 70, pp. 1015-1027, 2003.
[57] V. Cannillo, A. Corradi, C. Leonelli and A.R. Boccaccini. *A simple approach for determining the in situ fracture toughness of ceramic platelets used in composite materials by numerical simulations*. Journal of Materials Science Letters, 20, pp. 1889-1891, 2001.
[58] S. Hao, B. Moran, W.K. Liu and G.B. Olson. *A hierarchical multi-physics model for design of high toughness steels*. Journal of Computer-Aided Materials Design, 10, pp. 99-142, 2003.
[59] S. Choi and B.V. Sankar. *Fracture toughness of carbon foam*. Journal of Composite Materials, 37 (23), pp. 2101-2116, 2003.
[60] J.B. Choi and R.S. Lakes. *Nonlinear analysis of the Poisson's ratio of negative Poisson's ratio foams*. Journal of Composite Materials, 29 (1), pp. 113-128, 1995.